

## Binding energy of image-potential states: Dependence on crystal structure and material

K. Giesen, F. Hage, F. J. Himpsel,\* H. J. Riess, and W. Steinmann  
*Sektion Physik der Universität München, Schellingstrasse 4, D-8000 München 40,*  
*Federal Republic of Germany*  
 (Received 10 June 1986)

We have measured the binding energy of the image-potential states on Cu(100) and Ag(100) surfaces with two-photon photoemission spectroscopy. We find  $E_B = 0.57 (0.18) \pm 0.02$  eV for Cu(100) and  $0.53 (0.16) \pm 0.02$  eV for Ag(100) for the  $n=1$  ( $n=2$ ) states, respectively. These values are compared with the nearly hydrogenic binding energies of 0.77–0.83 eV obtained for the (111) surfaces of Cu, Ag, and Ni using the same method. The comparison shows that the binding energy does not depend on the material as long as the surface structure remains constant but changes markedly with the crystal orientation.

### I. INTRODUCTION

In the last few years image-potential states at metal surfaces have been studied extensively with the technique of inverse photoemission.<sup>1,2</sup> It turns out that the first member ( $n=1$ ) of the Rydberg-like series of these states has a binding energy of approximately 0.8 eV relative to the vacuum level. A Coulombic potential induced by the image charge of an electron outside the solid leads to a binding energy of roughly  $\frac{1}{16}$  Ry = 0.85 eV.<sup>1</sup> In this first approximation no individual properties of the sample are used (i.e., material or surface orientation), except the existence of a band gap of bulk states around  $E_{\text{vac}}$  which prevents the electron from escaping into the crystal. Using inverse photoemission spectroscopy one can measure the binding energy of the image potential states with an accuracy of about 150–200 meV. Within these experimental errors it is difficult to find any systematic trend in the binding energy when changing the material under investigation or the crystal orientation.<sup>1</sup>

An experimental method with an appreciably better energy resolution is required to detect a dependence of the binding energy on sample properties. Recently, we have developed the new experimental technique of high-resolution two-photon photoemission (2PPE) spectroscopy. In two preceding papers<sup>3,4</sup> we presented our data for the (111) surfaces of Cu, Ag, and Ni. We found that the binding energies of the  $n=1$  image potential states at the (111) surfaces are close to the hydrogenic value ( $E_B = 0.83, 0.77,$  and  $0.80$  eV for Cu, Ag, and Ni, respectively). In the present paper we report the results obtained with the (100) surfaces of Cu and Ag. This surface orientation exhibits a more pronounced surface corrugation. Furthermore, the position of the vacuum level is nearly midgap at the (100) surfaces, whereas it lies near the top of the gap at the (111) surfaces. Therefore it is of interest to see if one of these changes gives rise to a deviation of the binding energy from the hydrogenic value.

At the (111) surfaces of Cu, Ag, and Ni two-photon photoemission is a resonant process since an occupied surface state just below  $E_F$  is used as the initial state. A high

yield occurs if the exciting photon has an energy equal to the difference between the image potential state and the surface state.

At the (100) surfaces of Ag and Cu there is no occupied surface state just below  $E_F$ . Instead, the bulk  $\Delta_1$  band crosses the Fermi level, i.e., a continuum of bulk states exists both below and above  $E_F$  for  $k_{\parallel}=0$  (see Fig. 1). We demonstrate that two-photon photoemission can be observed even in the absence of an occupied surface state. In this case nonresonant processes dominate (see Fig. 1). Therefore, image potential states can be probed with two-photon photoemission for a very broad class of surfaces.

### II. EXPERIMENT

The experiments were performed with a frequency-doubled tunable dye laser pumped by a XeCl excimer laser with 10 ns pulse length. The light was  $p$ -polarized. No

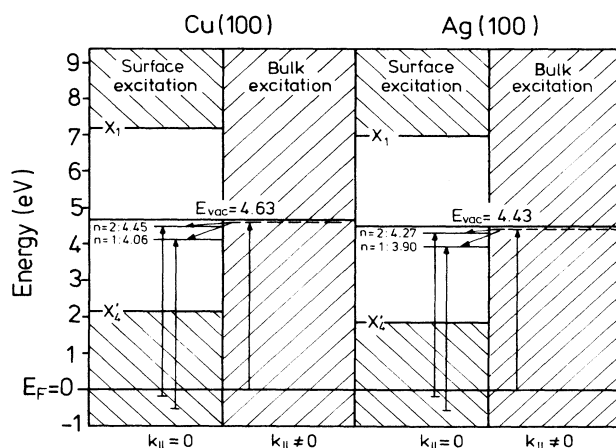


FIG. 1. Energy diagram for electronic states at the Cu(100) and Ag(100) surface. Hatched areas indicate projected bulk band continua. Several nonresonant processes can populate the  $n=1$  and 2 and image-potential states as indicated by arrows. The second photon ionizes the image-potential states.

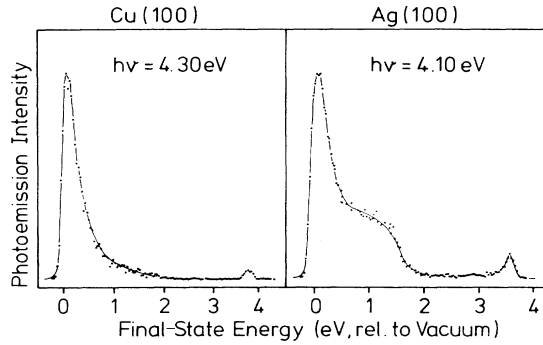


FIG. 2. Two-photon photoemission spectra from Cu(100) and Ag(100) at  $k_{\parallel}=0$ . Only the  $n=1$  state can be populated at the photon energies used.

emission was seen with  $s$  polarization, in agreement with selection rules for transitions from  $\Delta_1$  to  $\Delta_1$  states. Care was taken to avoid a distortion of the spectra by space-charge effects which turned on at about  $5 \times 10^4$  W/cm<sup>2</sup> power density. Heating of the sample by the laser light was negligible at this power. The photoelectrons were detected with an angle-resolving (narrower than  $\pm 2^\circ$ ) hemispherical energy analyzer capable of 50 meV energy resolution. The surfaces were cut to better than  $0.5^\circ$ , mechanically and electrochemically polished, and sputter-annealed in a  $2 \times 10^{-10}$  Torr vacuum. The zero of the energy scale of the energy distributions was determined by the turning point of the steplike low-energy cut-off of the one-photon photoelectron spectra taken with a rare-gas resonance lamp. By measuring the width of the one-photon spectra the work function of the samples could be determined with an accuracy of  $\pm 20$  meV:  $\phi = 4.42$  eV for Ag(100) and  $\phi = 4.63$  eV for Cu(100), in reasonable agreement with other authors.<sup>5-7</sup>

### III. RESULTS

Figure 2 shows the two-photon photoemission spectra of Ag(100) and Cu(100). The peak at the high-energy end of the spectra is much smaller than the zero-energy peak,

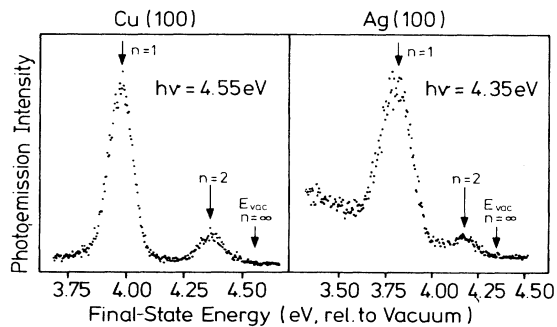


FIG. 3. Two-photon photoemission spectra from Cu(100) and Ag(100) at  $k_{\parallel}=0$ . The  $n=1$  and 2 states of the image-potential series are clearly resolved at higher photon energies.

TABLE I. Comparison of the binding energies for the five surfaces of Cu(111), Ag(111), Ni(111), Cu(100), and Ag(100), for which both inverse photoemission data and 2PPE data are available, as shown in Fig. 5. While the accuracy of the inverse photoemission data is not sufficient to clearly identify trends, the 2PPE data clearly show that the energy is independent of the material under investigation but changes drastically with the surface orientation.

	Binding energy (eV)		
	$n=1$	$n=2$	$n=3$
Cu(100)	$0.57 \pm 0.02$	$0.18 \pm 0.02$	
Ag(100)	$0.53 \pm 0.02$	$0.16 \pm 0.02$	
Ag(111)	$0.77 \pm 0.03$	$0.23 \pm 0.03$	$0.10 \pm 0.03$
Cu(111)	$0.83 \pm 0.03$		
Ni(111)	$0.80 \pm 0.03$		

while both peaks were of about the same height in the resonant spectra for the (111) surfaces (see Ref. 4). The weaker emission intensity for the image potential states at the (100) surfaces is due to the following. (i) Since there are no occupied surface states just below  $E_F$ , the image-potential state cannot be populated in a resonant transition. (ii) The initial state at the (100) surface is a bulk state. Therefore the transition matrix element to the image-potential states is smaller than at the (111) surfaces due to the reduced overlap of the wave functions.

For the Ag(100) surface an extra peak is observed at low electron energy (Fig. 2). A similar peak has been found in the 2PPE spectra from the Ag(111) surface and has tentatively been assigned to surface states on Ag(110) facets. The same assignment is offered for the low-lying peak observed at the Ag(100) surface.

Although the emission at the (100) surfaces is weaker, it is possible to resolve two members of the image-potential series as shown in Fig. 3. The binding energy of the image-potential states can be determined from the kinetic energy of the photoelectrons. When the photon energy is

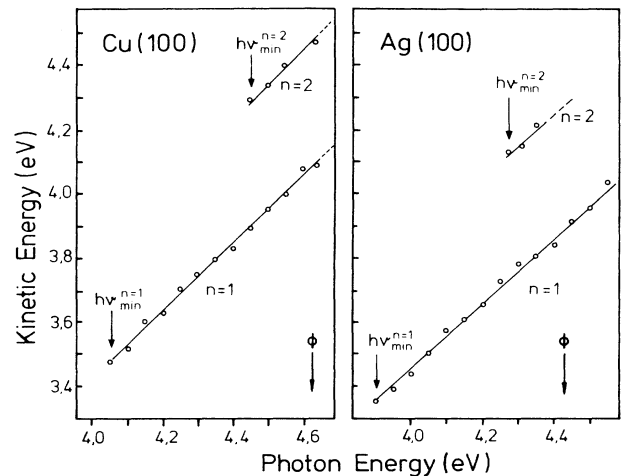


FIG. 4. Peak positions of  $n=1$  and 2 image-potential states of Cu(100) and Ag(100) vs photon energy.

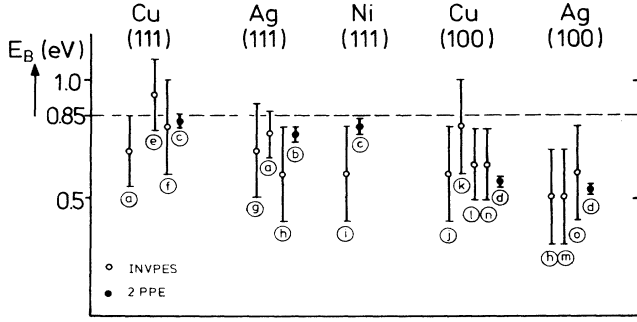


FIG. 5. Comparison of binding energies of image-potential states determined by inverse photoemission (open circles) and by two-photon photoemission (solid circles). *a*, Ref. 1; *b*, Ref. 3; *c*, Ref. 4; *d*, this work; *e*, Ref. 8; *f*, Ref. 9; *g*, Ref. 10; *h*, Ref. 11; *i*, Ref. 2; *j*, Ref. 12; *k*, Ref. 13; *l*, Ref. 8; *m*, Ref. 14; *n*, Ref. 15; *o*, Ref. 16.

increased, the peak position shifts by the same amount as  $h\nu$ . This is expected for a two-photon process with a fixed intermediate state. The binding energies  $E_B$  shown in Table I were determined by a least-squares fit of the experimental peak positions versus  $h\nu$  to a straight line (see Fig. 4):

$$E_{\text{kin}} = h\nu - E_B. \quad (1)$$

#### IV. DISCUSSION

The photoionization cross section of image-potential states has been calculated in the hydrogenic limit with the solid represented by a hard wall ("murium").<sup>17</sup> We can compare the second step in our 2PPE process with these calculations and thus obtain information about the first, more complicated step. Thereby, we learn about the population density of image states, which is of prime interest for future two-dimensional electron-gas experiments. We use the transition rates  $\Gamma_{E1}$  and  $\Gamma_{E2}$  calculated<sup>17</sup> for photoejection of an electron from the  $n=1$  and 2 states to the continuum:

$$\Gamma_{E1} = \frac{b \exp[-4\eta \tan^{-1}(1/\eta)]}{(1+\eta^2)^4}, \quad (2)$$

$$\Gamma_{E2} = \frac{2^4 b \exp[-4\eta \tan^{-1}(2/\eta)]}{(4+\eta^2)^4} \times \left[ 1 + \frac{4\eta^2}{4+\eta^2} \right]^2, \quad (3)$$

with

$$b \sim \frac{\eta^8}{1 - \exp(-2\pi\eta)},$$

$$\eta = 1/4ka_0,$$

$$k = \sqrt{2mE_{\text{kin}}}/\hbar,$$

$$a_0 = \text{Bohr radius}.$$

We obtain ratios  $\Gamma_{E1}/\Gamma_{E2} = 5.8$  (6.0) for the Cu(100) [Ag(100)] spectra shown in Fig. 3. The experimental area ratios are  $6 \pm 1$  ( $8 \pm 1$ ) for Cu(100) [Ag(100)]. The close agreement with the calculated ratios suggests that the population density in the  $n=1$  and 2 image states is comparable. Further evidence for an energy-independent population density comes from the observation that the intensity of the  $n=1$  state does not decrease significantly for finite  $k_{\parallel}$  (see subsequent paper), where we have additional kinetic energy of up to 0.4 eV. If there was thermal equilibrium (compare Ref. 18), a quasi-Fermi-level of 0.4 eV above the bottom of the two-dimensional image-state band would correspond to a population density of  $10^{-1}$  electrons per surface atom. Such a density is unreasonably high. Therefore we suspect that the electrons are not in thermal equilibrium.

Several theoretical models have been developed to account for deviations of the binding energy of the IPS's from the hydrogenic value.<sup>16,19</sup> Garcia *et al.* discuss the influence of surface corrugation (Fig. 5).<sup>16</sup> For Ag(100) they find that the  $n=2$  state is pulled down by the influence of the corrugation potential parallel to the surface and almost reaches the position of the unperturbed  $n=1$  state. In the case of the (111) surface we have shown<sup>4</sup> that this model cannot account for the different effective masses but equal binding energies of Cu, Ag, and Ni. According to Garcia *et al.* the binding energy is expected to increase with increasing corrugation. This trend is opposite to our observation, where the more corrugated (100) surfaces have a smaller binding energy than the less corrugated (111) surfaces.

Another attempt to describe the binding energy was made by Smith<sup>19</sup> (for details, see the following paper<sup>20</sup>) with a phase analysis based on earlier work of Echenique and Pendry.<sup>21,22</sup> In this theory image-potential states are subjected to the condition

$$\Phi_C + \Phi_B = 2\pi n, \quad n = 1, 2, 3, \dots \text{ for IPS's} \quad (4)$$

with  $\Phi_C$  the phase change of the electron wave function by reflection at the crystal and  $\Phi_B$  at the image-potential barrier.  $\Phi_C$  is dependent on the position within the band gap. For Cu and Ag we have  $\Phi_C(E_{\text{vac}}) \cong \pi$  at the (111) surface and  $\Phi_C(E_{\text{vac}}) \cong \pi/2$  at the (100) surface.<sup>23</sup> Taking  $\Phi_C$  to be constant over the range of the rydberg series, the binding energies  $E_B(n)$  of the individual members can be expressed by introducing a quantum defect  $a$ ,<sup>24</sup>

$$E_B(n) = (0.85 \text{ eV}) / (n+a)^2, \quad n = 1, 2, 3, \dots \quad (5)$$

The quantum defect  $a$  is correlated to the phase change  $\Phi_C$ .<sup>19,24</sup>

$$a = \frac{1}{2}(1 - \Phi_C/\pi). \quad (6)$$

For the (100) surface ( $\Phi_C \cong \pi/2$ ) the quantum-defect parameter  $a$  is about  $\frac{1}{4}$  and the binding energy  $E_B(n=1) \cong 0.54$  eV and  $E_B(n=2) = 0.17$  eV, in good agreement with our experimental data. For the (111) surface ( $\Phi_C \cong \pi$ ) the quantum defect parameter  $a$  is about 0

and hence the binding energies are given by the hydrogenic values  $E_B(n=1)=0.85$  eV and  $E_B(n=2)=0.21$  eV. Therefore, the phase-analysis model properly describes the trend in the experimental data of the binding energies measured with 2PPE.

#### ACKNOWLEDGMENTS

We would like to acknowledge X. Tang and R. Shakeshaft for providing unpublished results and R. Walkup for stimulating discussions.

\*Permanent address: IBM Thomas J. Watson Research Center, P.O. Box 218, Yorktown Heights, NY 10598.

<sup>1</sup>D. Straub and F. J. Himpsel, Phys. Rev. B **33**, 2256 (1986).

<sup>2</sup>A. Goldmann, V. Dose, and G. Borstel, Phys. Rev. B **32**, 1971 (1985).

<sup>3</sup>K. Giesen, F. Hage, F. J. Himpsel, H. J. Riess, and W. Steinmann, Phys. Rev. Lett. **55**, 300 (1985).

<sup>4</sup>K. Giesen, F. Hage, F. J. Himpsel, H. J. Riess, and W. Steinmann, Phys. Rev. B **33**, 5241 (1986).

<sup>5</sup>J. Hölzl and F. K. Schulte, in *Springer Tracts in Modern Physics* (Springer, Berlin, 1979) Vol. 85.

<sup>6</sup>P. O. Gartland, S. Berge, and B. J. Slagsvold, Phys. Norv. **7**, 39 (1973).

<sup>7</sup>M. Chelvayohan and C. H. B. Mee, J. Phys. C **15**, 2305 (1982).

<sup>8</sup>S. L. Hulbert, P. D. Johnson, N. G. Stoffel, W. A. Royer, and N. V. Smith, Phys. Rev. B **31**, 6815 (1985).

<sup>9</sup>W. Jacob, V. Dose, U. Kolac, Th. Fauster, and A. Goldmann, Z. Phys. B **63**, 459 (1986).

<sup>10</sup>S. L. Hulbert, P. D. Johnson, N. G. Stoffel, and N. V. Smith, Phys. Rev. B **32**, 3451 (1985).

<sup>11</sup>B. Reihl, K. H. Frank, and R. R. Schlittler, Phys. Rev. B **30**, 7328 (1985).

<sup>12</sup>W. Altmann, V. Dose, A. Goldmann, U. Kolac, and J. Rogo-

zik, Phys. Rev. B **29**, 3015 (1984).

<sup>13</sup>V. Dose, W. Altmann, A. Goldmann, U. Kolac, and J. Rogozik, Phys. Rev. Lett. **52**, 1919 (1984).

<sup>14</sup>B. Reihl, K. H. Frank, and R. R. Schlittler, Phys. Rev. B **30**, 7328 (1984).

<sup>15</sup>D. Straub and F. J. Himpsel, Phys. Rev. Lett. **52**, 1922 (1984).

<sup>16</sup>N. Garcia, B. Reihl, K. H. Frank, and A. R. Williams, Phys. Rev. Lett. **54**, 591 (1985).

<sup>17</sup>R. Shakeshaft and L. Spruch, Phys. Rev. A **31**, 1535 (1985), and private communication.

<sup>18</sup>J. Bokor, R. Haight, R. H. Storz, J. Stark, R. R. Freeman, and P. H. Bucksbaum, Phys. Rev. B **32**, 3669 (1985).

<sup>19</sup>N. V. Smith, Phys. Rev. B **32**, 3549 (1985).

<sup>20</sup>K. Giesen, F. Hage, F. J. Himpsel, H. J. Riess, W. Steinmann, and N. V. Smith, Phys. Rev. B **35**, 975 (1987), the following paper.

<sup>21</sup>P. M. Echenique and J. B. Pendry, J. Phys. C **11**, 2065 (1978).

<sup>22</sup>M. Ortúño and P. M. Echenique, Phys. Rev. B **34**, 5199 (1986).

<sup>23</sup>S. L. Hulbert, P. D. Johnson, M. Weinert, and R. F. Garrett, Phys. Rev. B **33**, 760 (1986).

<sup>24</sup>E. G. McRae, Rev. Mod. Phys. **51**, 541 (1979).